

# Microscopic Picture of Superfluid $^4\text{He}$

Yongle Yu<sup>†</sup> \* and Hailin Luo<sup>‡</sup>

<sup>†</sup> State Key Laboratory of Magnetic Resonance and Atomic and Molecular Physics, Wuhan Institute of Physics and Mathematics, Chinese Academy of Science, West No. 30 Xiao Hong Shan, Wuchang, Wuhan, 430071, China

<sup>‡</sup> Fujian Institute of Research on the Structure of Matter, Chinese Academy of Sciences, 155 Yangqiao Road West, Fuzhou, 350002, China

## Abstract.

We elucidate the microscopic quantum mechanism of superfluid  $^4\text{He}$  by uncovering a novel characteristic of its many-body energy levels. At temperature below the transition point, the system's low-lying levels exhibit a fundamental grouping behavior, wherein each level belongs exclusively to a single group. In a superflow state, the system establishes thermal equilibrium with its surroundings on a group-specific basis. Specifically, the levels of a selected group, initially occupied, become thermally populated, while the remaining groups of levels stay vacant due to absence of transitions between groups. The macroscopic properties of the system, such as its superflow velocity and thermal energy density, are statistically determined by the thermal distribution of the occupied group. Additionally, we infer that the thermal energy of a superflow has an unusual relationship with flow velocity, such that the larger the flow velocity, the smaller the thermal energy. This relationship is responsible for a range of intriguing phenomena, including the mechano-caloric effect and the fountain effect, which highlight a fundamental coupling between the thermal motion and hydrodynamic motion of the system. Furthermore, we present experimental evidence of a counterintuitive self-heating effect in  $^4\text{He}$  superflows, confirming that a  $^4\text{He}$  superflow carries significant thermal energy related to its velocity.

## I. Introduction

The discovery of quantum mechanics represents a paradigm shift in the evolution of modern civilization. It not only deepens our understanding of physical systems at a fundamental level but also drives the development of numerous vital technologies that have permeated all aspects of human life.

Quantum mechanics offers a unified framework for describing diverse physical systems, ranging from atomic and molecular systems to condensed matter systems

\* Email-address: yongle.yu@wipm.ac.cn

and beyond, despite its counterintuitive features such as quantum entanglement and tunneling. According to the theory's formulation, the physical states of any given system can be characterized by a set of quantum wavefunctions (states) of the system, and the physical processes associated with the system correspond to the transitions between these quantum states.

The field of atomic and molecular physics has achieved remarkable success in attaining a high degree of accuracy in the quantitative agreement between quantum theory and experimental observations. This can be attributed, in part, to the relatively small number of particles involved in these systems, enabling precise calculations of their quantum properties. However, in condensed matter physics, the quantitative agreement between quantum theory and experimental data is often less satisfactory, with even qualitative understanding proving elusive in some instances. This is primarily due to the quantum many-body problem, which is associated with a large number of particles in the corresponding system. To tackle this challenge, quantum approximations, such as the mean field or single-particle approach, are commonly employed. This approach approximates the quantum state of a system using a product of single-particle quantum wavefunctions and can explain significant phenomena, such as the distinctions between conductors, semiconductors, and insulators.

Despite its widespread use, the single-particle approach has proved inadequate in addressing several intriguing quantum phenomena. Notably, there are exceptions to this method, such as the Laughlin wavefunction, which is used to describe the fractional quantum Hall effect.

Superfluid  $^4\text{He}$  is one of the most fundamental condensed matter systems, which exhibits a wide variety of unusual quantum behaviors. The phenomenon of superfluidity [1, 2], characterized by the absence of dissipation, is seemingly somehow at odds with the second law of thermodynamics, which typically dictates that a closed system will reach a thermal state of maximum entropy by converting all energy of an ordered motion into thermal energy. Several phenomena of superfluid  $^4\text{He}$ , such as the fountain effect [3] and the mechano-caloric effect [4], reveal an intriguing coupling between the hydrodynamic and thermal motions of the system. A naturally posed question is whether one can understand these unusual behaviors in the direct terms of quantum states and quantum transitions among them. Is it possible to form a quantum picture of superfluid  $^4\text{He}$  which is as clear and straightforward as that of an atomic system? The present paper seeks to provide an affirmative answer to this question.

We present some general physical arguments which lead to a novel grouping behavior of low-lying many-body levels of superfluid  $^4\text{He}$  at low temperature, with each level belonging exclusively to one single group. The system establishes a group-specific thermal equilibrium with its surroundings, and depending on the group occupancy, it can sustain a macroscopic superflow state. Moreover, we demonstrate that the grouping of its low-lying levels give rise to an intriguing property, namely, a velocity-dependent thermal energy for the superflow. Specifically, as the velocity of the superflow increases, the thermal energy decreases. This velocity-dependent behavior is responsible for the

fundamental coupling between the hydrodynamic and thermal motions of the system.

There are numerous important theoretical works in the literature that provide significant insights into various aspects of superfluid  $^4\text{He}$  (see, for example, [5, 6, 7, 8, 9, 10, 11, 12, 13] and the references in [14]). It is worth noting that the present theoretical advancement owes much to the inspirations from some of these seminal works.

The rest of paper is organized as follows. In Section II, we present a critical analysis of the two-fluid model superfluid  $^4\text{He}$ , highlighting a fundamental inadequacy in this phenomenological model. We also discuss several experimental observations that contradict the two-fluid model, emphasizing the need for a direct microscopic picture of the system. In Section III, we illustrate some general properties of the quantum states of superfluid  $^4\text{He}$ , with particular attention to the grouping behavior of its low-lying levels. Section IV argues that the thermal energy of superfluid  $^4\text{He}$  naturally depends on the flow velocity due to the properties of the occupied group(s) and the properties of Galilean transformation. In Section V, we report an intriguing self-heating phenomenon of  $^4\text{He}$  superflows, providing evidence that superflow  $^4\text{He}$  can carry significant thermal energy depending on the flow velocity. Finally, we provide our conclusions and perspectives in Section VI.

## II. Fundamental inadequacy of the two-fluid model and its inconsistency with experimental observations.

The two-fluid model of superfluid  $^4\text{He}$  is essential to the textbook understanding of numerous behaviors of the system. However, this phenomenological model has a fundamental inadequacy that poses a significant challenge to its reliability.

The two-fluid model postulates the existence of a superfluid component that possesses an exotic characteristic of zero entropy. With this postulation, the superfluid component is considered a thermodynamic sub-system, allowing for the investigation of its temperature. However, maintaining consistency with the zero entropy assumption requires this temperature to be absolute zero, which raises the fundamental question of how this zero-temperature component can coexist with its thermal surroundings. This would be more 'miraculous' than spotting ice in molten steel, and the zeroth law of thermodynamics unequivocally rules out such coexistence. In contrast, we shall demonstrate subsequently that the microscopic mechanism of superfluidity is free from unrealistic assumptions of zero entropy and adheres to the zeroth law of thermodynamics.

There exists another unnaturalness in the two-fluid model. According to this model, the sum of the normal and the superfluid densities remains constant, corresponding to the total density of all  $^4\text{He}$  atoms in the system. The normal density is determined by computing the density of quasiparticles, such as phonons and rotons, with each quasiparticle corresponding exactly to one  $^4\text{He}$  atom in the total density. By subtracting the quasiparticle-mapped atoms, the remaining  $^4\text{He}$  atoms constitute the superfluid component. It is clear that the concept of two components corresponds to a bipartition

of  $^4\text{He}$  atoms in the system. However, this bipartition is not supported at a fundamental level. In accordance with principles of quantum mechanics, the microscopic states of the system are specified by a large number of many-body wavefunctions. These wavefunctions, denoted by  $\psi_\alpha(\mathbf{r}_1, \mathbf{r}_2, \dots, \mathbf{r}_N)$ , can be conveniently taken as the eigenstates of the Hamiltonian operator of the system, with  $\alpha$  labeling the eigen levels and  $N$  denoting the total number of atoms. Within these wavefunctions, all the atoms must be treated as an indivisible entity, possessing complex intrinsic quantum correlations among them due to the inter-atomic interactions.

In previous studies, several experimental observations have directly contradicted the predictions of the two-fluid model. This result is not entirely surprising, as the main assumption of the two-fluid model is subjective in nature.

Two experimental studies [15, 16] have investigated the behavior of meniscus of superfluid  $^4\text{He}$  in a rotational bucket. According to the two-fluid model, only the normal component should rotate, while the superfluid component remains stationary. As a result, only normal component generates a meniscus, and its height is expected to be proportional to the normal density, leading to an increase with temperature and vanishing at low temperatures.

However, the experimental findings are contrary to these predictions. Specifically, the height of the meniscus remains constant with temperature, and its value seems to suggest that the entire system is composed of the normal component, independent of temperature.

Consequently, the height of the meniscus is expected to increase with temperature and vanish at the low temperatures. However, the experimental findings are contrary to these predictions. Specifically, the height of the meniscus remains unaltered with temperature, and its value indicates that entire comprises the normal component, independent of temperature. Furthermore, The experiment [16] demonstrates that the rotating  $^4\text{He}$  exhibits the thermo-mechanical effect, which contradicts the conclusion that the system is solely composed of the normal component.

A different set of experiments explores the oscillation and attenuation of superflow motion between two containers of superfluid  $^4\text{He}$  within the same isothermal enclosure [17, 18, 19, 20, 21, 22, 23]. By positioning the liquid levels in the containers differently, a superflow motion, typically in the form of mobile surface film, can be generated through gravitational potential difference. When the liquid levels are equalized, the inertial in the superflow subsequently cause the levels to oscillate about the equilibrium position. the attenuation of liquid level oscillations is discernible, indicative of the dissipation of gravitational potential energy.

Investigating the temperature dependence of the damping rate of is of particular interest. According to the two-fluid model, the normal component causes the dissipation. Therefore, as the ratio of normal component approaches zero in the low temperature limit, the damping rate shall also vanish. However, the experimental observations show that the damping rate remains finite and relatively large in the low temperature limit.

A similar behavior is also observed in superconductors. In an experiment

study[24, 25], the  $Q$  value of a microwave cavity made of superconductor niobium is measured. According to the two-fluid model, it is expected that the  $Q$  value would increase exponentially as the temperature approaches absolute zero. However, experimental measurements indicate that the  $Q$  value approaches a constant value below the temperature of 1.3  $K$ .

The dissipation behavior of superfluid  $^4\text{He}$  and superconductors is considered an open question in literature. Later in this work, we demonstrate a natural explanation for this phenomenon and argue that the assumption of dissipationless behavior in superfluid systems cannot always be taken for granted.

The two-fluid model proposes that a  $^4\text{He}$  superflow carries no thermal energy, which appears to be supported by various experimental observations. However, These experiments lack effective control of the superflow velocity, and the negligible thermal energy density of a superflow is associated with a large velocity. In Section V, we present an experiment in which the superflow velocity is partially regulated, and we demonstrate that a superflow can indeed carry significant thermal energy, resulting in a counter-intuitive heating phenomenon. This experimental result directly contradicts the pivotal hypothesis of the two-fluid model.

The aforementioned limitations of the two-fluid model demonstrate its inability to offer a comprehensive account of superfluid  $^4\text{He}$ . It is necessary to develop a full quantum microscopic description of the superfluid  $^4\text{He}$  in order to establish a reliable, inherent, and unified understanding of the system.

### III. Grouping behavior of low-lying levels of superfluid $^4\text{He}$

We consider a liquid  $^4\text{He}$  system which is periodic and translationally invariant along the  $x$  axis, and is constrained in the  $y, z$  directions by the inner boundary of a container (see Fig. 1). The length of the system in the  $x$  direction is  $L$ . The Hamiltonian of the system can be written as

$$\widehat{H} = \sum_{i=1}^N -\frac{\hbar^2}{2M} \nabla_i^2 + \sum_{i<j}^N V(\mathbf{r}_i - \mathbf{r}_j), \quad (1)$$

where  $M$  is the mass of a  $^4\text{He}$  atom,  $\hbar$  is the reduced Plank constant,  $N$  is the total number of the atoms and  $V$  is the interaction between two atoms.

The eigen-wavefunctions of the Hamiltonian operator are governed by the following equation,

$$\widehat{H}\psi_\alpha(\mathbf{r}_1, \mathbf{r}_2, \dots, \mathbf{r}_N) = E_\alpha\psi_\alpha(\mathbf{r}_1, \mathbf{r}_2, \dots, \mathbf{r}_N), \quad (2)$$

where  $\alpha$  labels the eigen-wavefunctions and  $E_\alpha$  is the eigen energy of the state.

Given that  $\widehat{H}$  commutes with the total momentum operator  $\widehat{P}_x = -\hbar \sum_{j=1}^N \frac{\partial}{\partial x_j}$  (along the  $x$  axis), it follows that the eigen-wavefunctions of  $\widehat{H}$  can be chosen to be the eigen-wavefunctions of the  $\widehat{P}_x$  simultaneously

$$\widehat{P}_x\psi_\alpha(\mathbf{r}_1, \mathbf{r}_2, \dots, \mathbf{r}_N) = P_\alpha\psi_\alpha(\mathbf{r}_1, \mathbf{r}_2, \dots, \mathbf{r}_N), \quad (3)$$

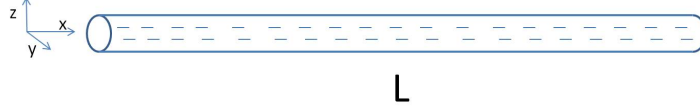


**Figure 1.** The geometry of a liquid  $^4\text{He}$  system with a periodic length of  $L$  in  $x$  direction ( $x$  is identical to  $x + L$ ).

where  $P_\alpha$  is the eigen momentum.

For a given eigen-wavefunction  $\psi_\beta(\mathbf{r}_1, \mathbf{r}_2, \dots, \mathbf{r}_N)$  with an energy of  $E_\beta$  and a momentum of  $P_\beta$ , additional eigen-wavefunctions can be constructed by applying a Galilean transformation, which captures center-of-mass motion. The transformed wavefunction is obtained by,

$$\psi_\beta^{cm_k}(\mathbf{r}_1, \mathbf{r}_2, \dots, \mathbf{r}_N) = e^{i \sum_{j=1}^N 2\pi k x_j / L} \psi_\beta(\mathbf{r}_1, \mathbf{r}_2, \dots, \mathbf{r}_N), \quad (4)$$

where  $k = \pm 1, \pm 2, \pm 3, \dots$ , is an interger.

The energy and momentum associated with  $\psi_\beta^{cm_k}$  can be determined by,

$$E_\beta^{cm_k} = E_\beta + (P_\beta + 2\pi k N \hbar / L)^2 / (2NM) - P_\beta^2 / (2NM) \quad (5)$$

and

$$P_\beta^{cm_k} = P_\beta + 2\pi k N \hbar / L. \quad (6)$$

Eqs. (4), (5) and (6) reflect the Galilean invariance of the system [11].

We shall study investigate the system's low-lying levels which are the relevant levels at low temperature. Due to the exponential Boltzmann factor, the contribution of high-lying levels is negligible.

A grouping behavior of the low-lying levels can be revealed by a fundamental analysis of quantum transitions between these levels. These quantum transitions also play an essential role in the thermalization of the system. The microscopic atomic-molecular interactions between the system and its surroundings cause frequent momentum-energy exchanges and drive the quantum transitions between the system's low-lying levels, ultimately leading to a thermal occupations of its levels.

Formally, the transition probability from one level with an eigen-wavefunction  $\psi_i(\mathbf{r}_1, \mathbf{r}_2, \dots, \mathbf{r}_N)$  to another level with an wavefunction  $\psi_j(\mathbf{r}_1, \mathbf{r}_2, \dots, \mathbf{r}_N)$  is determined through one particle scattering process as follow,

$$P_{\psi_i \rightarrow \psi_j} = |\langle \psi_j(\mathbf{r}_1, \mathbf{r}_2, \dots, \mathbf{r}_N) | \sum_{m,l=0,\pm 1,\dots} f(m-l) a_m^\dagger a_l | \psi_i(\mathbf{r}_1, \mathbf{r}_2, \dots, \mathbf{r}_N) \rangle|^2, \quad (7)$$

where  $a_l$  is the annihilation operator corresponding to a single-particle orbit which carries an eigen momentum of  $2\pi l \hbar / L$  along  $x$ -direction (the wavefunction of the orbit has a  $x$ -dependence of  $e^{i2\pi l x / L}$ , the  $y, z$ -dependence of the orbit is ignored for simplicity),  $a_m^\dagger$  is the creation operator for a single-particle orbit with a wavefunction of  $e^{i2\pi m x / L}$ , and the function  $f(m-l)$  describes the strength of the scattering.

Depending on these two levels,  $P_{\psi_i \rightarrow \psi_j}$  can easily vanish. In some instances it may assume an exact value of zero, whereas in the realistic case, it vanishes in the sense that its value decreased exponentially as a function of  $N$ . Whether or not  $P_{\psi_i \rightarrow \psi_j}$  vanishes is dependent on the degree of proximity between the two corresponding wavefunctions. For instance, let  $\psi_i$  have a Bose-Einstein condensation (BEC) form which is associated with a single-particle orbit  $|\phi_1\rangle$  with a wavefunction of  $\phi(y, z)e^{i2\pi x/L}$ , such that  $\psi_i(\mathbf{r}_1, \mathbf{r}_2, \dots, \mathbf{r}_N) = |\phi_1^N\rangle$ . Similarly, let  $\psi_j$  represent the BEC of another single-particle orbit  $|\phi_2\rangle = \phi(y, z)e^{i4\pi x/L}$ , resulting in  $\psi_j(\mathbf{r}_1, \mathbf{r}_2, \dots, \mathbf{r}_N) = |\phi_2^N\rangle$ . It can be shown easily that  $P_{\psi_i \rightarrow \psi_j}$  is exactly zero. Furthermore, consider  $\psi_i(\mathbf{r}_1, \mathbf{r}_2, \dots, \mathbf{r}_N) = |\phi_1^{M_1} \phi_2^{N-M_1}\rangle$  (where  $M_1$  particles occupy orbit  $\phi_1$  and  $N-M_1$  particles occupy orbit  $\phi_2$ ,  $M_1 \leq N$ ), and that  $\psi_j(\mathbf{r}_1, \mathbf{r}_2, \dots, \mathbf{r}_N) = |\phi_1^{M_2} \phi_2^{N-M_2}\rangle$ ,  $P_{\psi_i \rightarrow \psi_j}$  always vanishes unless  $|M_1 - M_2| \leq 1$ . Here, the degree of difference between  $|\phi_1^{M_1} \phi_2^{N-M_1}\rangle$  and  $|\phi_1^{M_2} \phi_2^{N-M_2}\rangle$  can be roughly approximated as  $|M_1 - M_2|$ , which is the difference of number of particles occupying a major orbit. These straightforward observations suggest that the transition probability between two quantum states associated with partial BEC is negligible, unless they have almost an equal number of particles to occupy the same orbit.

We shall consider the ground state wavefunction of the system  $\psi_g(\mathbf{r}_1, \mathbf{r}_2, \dots, \mathbf{r}_N)$  which has the ground state energy  $E_g$  ( $\hat{H}|\psi_g\rangle = E_g|\psi_g\rangle$ ) and has a zero momentum along  $x$  axis ( $P_x|\psi_g\rangle = 0$ ). One can obtain another eigenstate which is a Galilean transformation of the ground state  $\psi_g^{cm1}(\mathbf{r}_1, \mathbf{r}_2, \dots, \mathbf{r}_N) = e^{i\sum_{j=1}^N 2\pi x_j/L} \psi_g(\mathbf{r}_1, \mathbf{r}_2, \dots, \mathbf{r}_N)$ . The transition probability between these two states is given by,  $P_{\psi_g \rightarrow \psi_g^{cm1}} = |\langle \psi_g | \sum_{m,l} f(m-l) a_m^\dagger a_l | \psi_g^{cm1} \rangle|^2$ . It can be argued that  $P_{\psi_g \rightarrow \psi_g^{cm1}}$  vanishes naturally. First, the momentum difference between these states is  $2\pi N\hbar/L$ , which is large from a microscopic perspective. For such a transition to occur, it would require a scattering process involving single-particle orbits with large momentum. However, for the ground state, which can be written as a supposition of Fock states in momentum space, its component involving a single-particle orbit of large momentum is negligible, as the engagement of large momentum (single-particle) orbit costs high kinetic energy, which is unfavorable to the ground state. As a result, the scattering amplitude vanishes. Secondly, the ground state is expected to exhibit strong correlation of  $^4\text{He}$  atoms. It is difficult to precisely describe this correlation, but a substantial portion of it is manifested by a partial BEC in the wavefunction [8, 9, 10]. The condensate fraction of ground state is estimated to be around 10% in the literature [26, 27, 28, 29, 30, 31, 32, 33, 34, 35, 36, 37, 38, 39, 40, 41]. For convenience, If a many-body eigenstate involves a partial BEC, the single-particle orbit required to accommodate this BEC is referred to as the base orbit of the state. It is apparent that base orbit of  $\psi_g$  possesses a zero momentum along  $x$ -direction. On the other hand,  $\psi_g^{cm1}$  corresponds to an Galilean transformation of  $\psi_g$ , while the internal correlations of the atoms are unaffected by the transformation. However, the base orbit of  $\psi_g^{cm1}$  has eigen momentum value of  $2\pi\hbar/L$ , and it is orthogonal to the base orbit of  $\psi_g$ . According to the previous discussion, there is a large degree of difference between  $\psi_g^{cm1}$  and  $\psi_g$ ; therefore,  $P_{\psi_g \rightarrow \psi_g^{cm1}}$  shall vanish.

Not only the ground state, but also all low-lying eigen states possess the same type of correlation, which is manifested in a crude form of a partial BEC [30, 31, 34, 35, 37, 38, 39, 41]. This correlation is primarily owing to the effect of Bose exchange interaction [42]. If a quantum state involves a condensate fraction, the energy of the Bose exchange interaction can be significantly reduced. In contrast, for an eigen state without a condensate fraction, the exchange interaction substantially raises its energy, excluding it from the low energy regime.

Following the preceding analysis, a grouping behavior for low-lying levels arises naturally. Specifically, the levels sharing base orbit are categorized together, forming a group separate from other groups comprised of levels with different base orbits.

The group involving the ground state  $\psi_g$  is denoted as  $grp_0$ , while the group incorporating  $\psi_g^{cm_1}$  is labeled as  $grp_1$ . It is evident that  $grp_1$  can be viewed as a Galilean transformation of  $grp_0$ . Likewise,  $grp_k$  ( $k = 2, 3, \dots$ ) can be obtained by multiplying all eigen wavefunctions in  $grp_0$  by a Galilean factor of  $e^{i \sum_{j=1}^N 2\pi k x_j / L}$ . The group  $grp_{-|k|}$  with a negative integer value of  $k$  can be formed by applying a corresponding Galilean factor.

For any two levels ( $\psi_a$  and  $\psi_b$ ) in the same group, it is always to find a chain of levels ( $\psi_n (n = 1, 2, \dots, N^c)$ ) in this group such that all the transition probabilities  $P_{\psi^a \rightarrow \psi_1}, P_{\psi_1 \rightarrow \psi_2}, P_{\psi_2 \rightarrow \psi_3}, \dots, P_{\psi_{N^c-1} \rightarrow \psi_{N^c}}, P_{\psi_{N^c} \rightarrow \psi_b}$  do not vanish. In other words,  $\psi_a$  can be eventually scattered to  $\psi_b$  through a series of scattering processes. However, if two levels belong to two different groups, it is not possible to find a series of scattering processes which connects these two levels unless some high-lying levels are involved.

At low temperature, the system can establish a group-specific thermal equilibrium with its surroundings. For instance, when some levels of a particular group are initially occupied, the frequent quantum exchanges between the system and its surroundings shall lead to dispersion of the level occupations, eventually resulting in a thermal population of all levels in the group. On the other hand, Those groups which were initially unoccupied remain unoccupied, as the inter-group transition is prohibited by the presence of high energy barriers.

Some levels in  $grp_0$ ,  $grp_1$  and  $grp_2$  are schematically plotted in the momentum energy plane in Fig. 2. The lower boundaries (the many-body dispersion lines) of  $grp_0$  are roughly linear in both positive and negative momentum directions, and the slopes of two linear disperions are of equal magnitude [42, 43, 7, 11]. In  $grp_1$ , the slope magnitude of positive linear dispersion is larger than slope magnitude of negative linear branch, this is because that Galilean transformation of a positive linear dispersion line (in the positive  $P$  direction) makes the line more titled, whereas it makes the line less titled in the case of negative linear dispersion. in the case of  $grp_2$ , the slope magnitude of the positive linear dispersion line increases further. Note that  $grp_0$  and  $grp_1$  are overlapped in some regions, with the overlap being more prevalent in the upper region of higher energy. The overlap of these two groups might give rise to a false impression that quantum jumps between them are possible. As analyzed earlier, every wavefunction in  $grp_0$  has a large degree of difference from the wavefunctions in  $grp_1$  due to their distinct



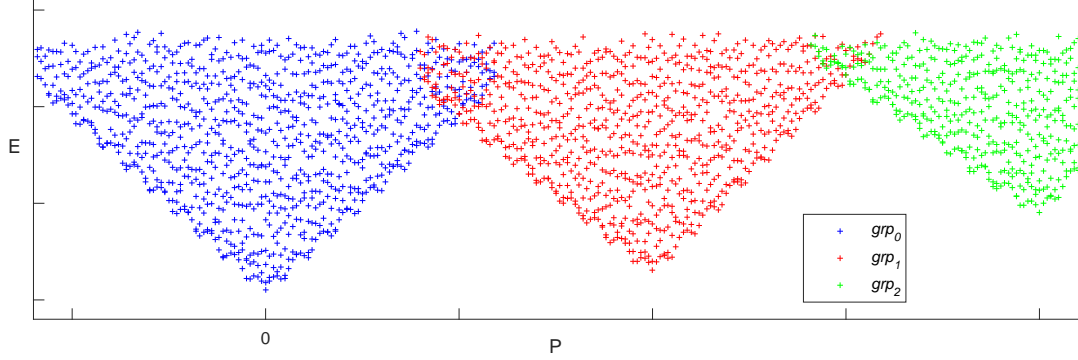


**Figure 2.** A schematic plot of some low-lying levels of  $grp_0$ ,  $grp_1$  and  $grp_2$ , labeled in color, in the momentum energy plane. Each level is marked by a plus sign. The groups overlap in some regions in the plane, and the extent of their overlaps increases in regions of high energy (not shown in the figure).

base orbits, consequently, the transition probability between them vanishes.

The phenomenon of superfluidity can be naturally explained based on the grouping of the levels. If only  $grp_0$  is initially occupied, the average momentum of the system at thermal equilibrium is zero, indicating a static state. Assuming, for instance,  $grp_2$  is exclusively occupied at the outset, the average momentum of the system at thermal equilibrium can be determined statistically by the following equation:

$$\overline{P}_{grp_2}^T = \frac{\sum_{\phi_\gamma \in grp_2} \langle \phi_\gamma | \widehat{P}_x | \phi_\gamma \rangle e^{\frac{-E_\gamma}{kT}}}{\sum_{\phi_\gamma \in grp_2} \langle \phi_\gamma | \phi_\gamma \rangle e^{\frac{-E_\gamma}{kT}}}. \quad (8)$$

A non-zero value of  $\overline{P}_{grp_2}^T$  indicates the presence of a persistent current in the system.  $\overline{P}_{grp_2}^T$  possesses a temperature dependence due to the Boltzmann factor in Eq. 8. If the temperature of the system undergoes a gradual change followed by a return to its initial value,  $\overline{P}_{grp_2}^T$  will vary accordingly and eventually revert to its initial value. Such a temperature dependence is largely confirmed by an experiment [44] in the past.

In reality, the translational invariance of a superfluid  $^4\text{He}$  system is imperfect. For example, the irregularities in the inner wall of the container can disrupt the exact translational symmetry. Nonetheless, this symmetry-broken interaction, or potential, can be considered a minor perturbation term when compared to terms in Eq. 1 (The atomic-molecular interactions between the system and the container are confined to a few layer of  $^4\text{He}$  atoms near the wall, and the interaction strength decreases quickly as a  $^4\text{He}$  atom moves away from the wall surface). Although the microscopic many-body wavefunctions are no longer the eigenstates of  $\widehat{P}_x$ , one can use the expectation value of this operator for theoretical purposes. In higher order treatment, this perturbation term might mix the levels of the same group by an infinitesimal amount, but it is not

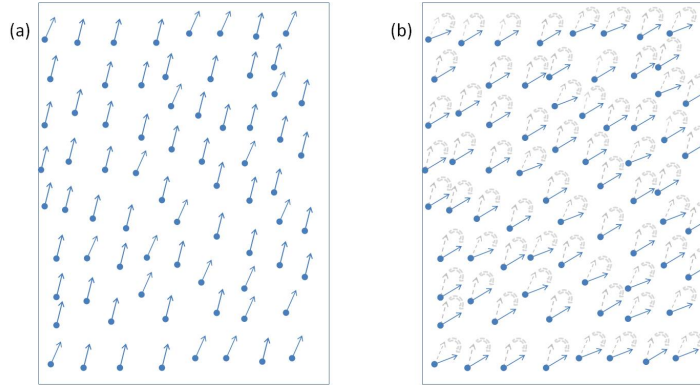


**Figure 3.** a) In a ferromagnet, the microscopic magnetic moments (spins) roughly align in the same direction. b) A smooth transition between two metastable states is only possible if all the microscopic moments rotate collectively, which generally requires an external manipulation.

sufficient to mix two levels which belong to two distinct groups. Inter-group mixing can only occur if the perturbation term has a homogeneous influence on all atoms in the system. Therefore, it can be concluded that the grouping behavior of microscopic levels remains quite robust regardless of an exact translational symmetry.

The grouping behavior of low-lying levels in superfluid  $^4\text{He}$  is of full quantum nature. It is related to a particular property of each low-lying level (the corresponding wavefunction has a condensate fraction), as well as transition probabilities among these levels. Although it was unnoticed in the past, one can realize that the grouping of microscopic levels is not unique to a superfluid system. For instance, consider a ferromagnet for an illustration. Below the Curie point, the microscopic magnetic moments (spins) in the ferromagnet tend to align approximately in the same direction (see Fig. 3(a)). The system possesses numerous macroscopic states due to the different directions of total magnetic moments, and each of these states corresponds to a specific group of microscopic levels. The metastability of each macroscopic state can be attributed to the following factors. i) The thermal transition between any two distinct groups of microscopic levels is impossible at low temperatures since such a transition requires overcoming a high energy barrier that separates the groups. ii) A smooth transition between two different groups of levels is possible if all spins rotate simultaneously by the same angle (see Fig. 3(b)). This collective motion of all spins involved in such a transition does not encounter a high energy barrier. However, this collective motion cannot initiate spontaneously and requires some form of external operation, such as the application of a strong magnetic field. It should be noted that in the case of superfluid  $^4\text{He}$ , a smooth transition between different groups of levels can occur under the influence of a global force. For instance, the application of a force, such as gravity or hydrodynamic pressure, that acts uniformly on all  $^4\text{He}$  atoms and accelerate them collectively can establish such a transition.

In the context of the analogy between the superfluid  $^4\text{He}$  and a ferromagnet, a

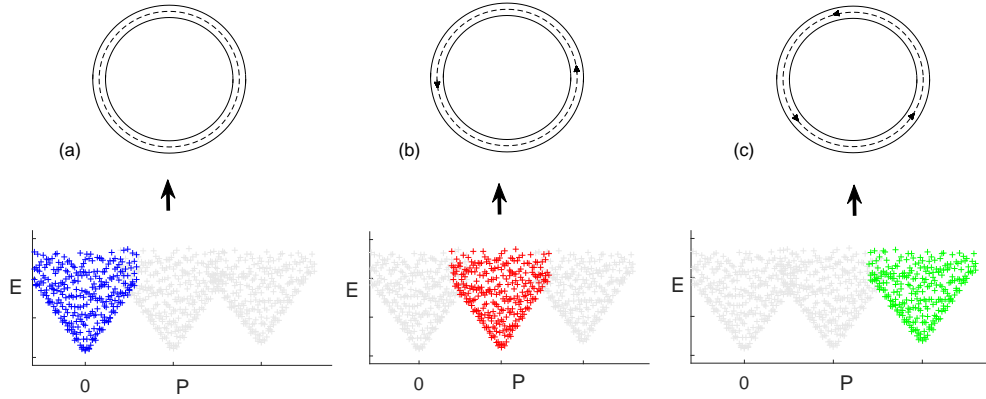


**Figure 4.** A schematic plot of macroscopic-microscopic correspondence that underlies the metastability of  $^4\text{He}$  superflows. (a) represents a static state, while (b) and (c) show superflow states with small and slightly larger velocities, respectively. The occupied groups are highlighted in color.

broader perspective on the grouping of the microscopic can be formed. In such systems, two fundamental facts are observed: i) the existence of a number of macroscopic metastable states at low temperatures; and ii) a large number of microscopic low-lying levels. Establishing a connection between these two facts shall naturally lead to the realization that the low-lying levels of the system are organized into groups, physically separated by some high energy barriers. In this way, a macroscopic metastable state corresponds to a group of microscopic levels (such a macroscopic-microscopic correspondence resolves the mystery of superfluidity in a transparent way, see Fig. 4). On the other hand, at sufficiently high temperatures, the energy barriers are overcome and all groups of low-lying levels are thermally occupied along with the relevant high-lying levels, resulting in a reduction of the number of the macroscopic thermal states to one.

The preceding discussions can be readily generalized to other condensed matter systems that exhibit low temperature phases characterized by an order parameter. The microscopic quantum pictures of these systems share the following features: i) there exists a grouping behavior of the low-lying levels in each system, where the occupancy of a specific group and the vacancy of other groups correspond to a metastable state with a certain order parameter value that is statistically determined by the occupied group; ii) a smooth inter-group transition at low temperature might be feasible if a suitable collective motion of all particles in the system occurs, but such collective motion is not guaranteed. Inter-group transitions through spontaneous thermal excitations are prohibited since they involve high-lying levels that are effectively irrelevant at low temperatures; iii) as the temperature rises above the transition point, the grouping of low-lying levels becomes

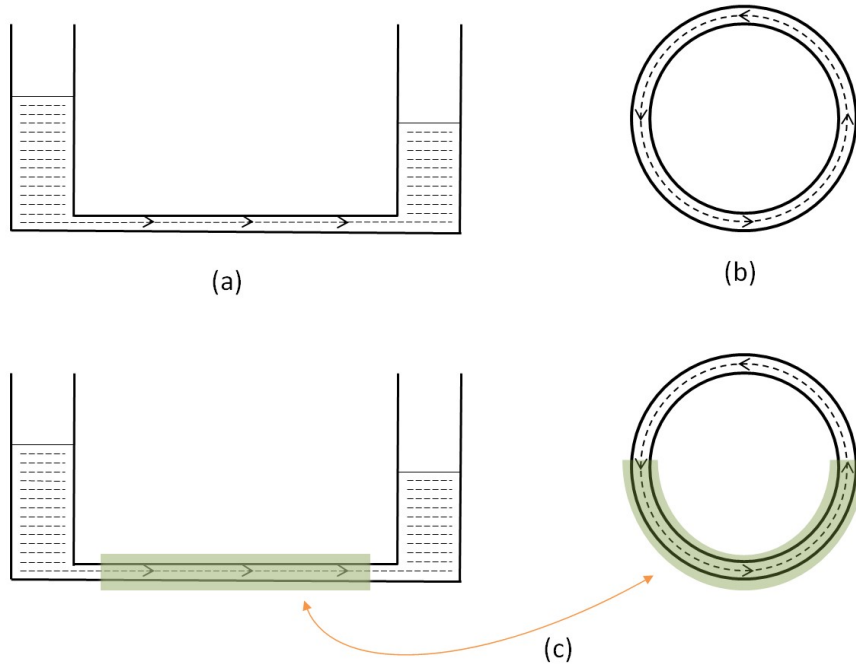


**Figure 5.** (a) an open superflow system of  $^4\text{He}$  which connects to two vessels. (b) a close superflow system with a natural periodic system. (c) The systems within the colored shaded areas are equivalent to each other.

irrelevant, and inter-group transitions become possible through thermal excitations involving high-lying levels, which are more abundant and statistically more significant than the low-lying levels, leading the system to a single thermal state with an order parameter value of zero.

We shall explain why superfluid  $^4\text{He}$  is not dissipationless in certain cases (some relevant experiments were discussed in Section II). The dissipationless behavior of superfluid  $^4\text{He}$  is predicated on its attainment of group-specific thermal equilibrium, which is manifested by a steady flow motion. However, when the superflow oscillates between two vessels, there is frequent microscopic inter-group transitions caused by a global force which drives all  $^4\text{He}$  atoms in the flow. As a result, numerous groups of low-lying levels become intermittently occupied and unoccupied over time, which precludes the superflow from reaching thermal equilibrium. Inevitably, dissipation arises during these microscopic transition processes, and the system behaves similarly to a normal system regarding the temperature-dependent dissipation rate at low temperature limits.

In order to facilitate a thorough understanding of the fundamental properties of superfluid  $^4\text{He}$ , it is useful to reflect on one of the theoretical conditions that is involved in the discussions. It has been shown that the low-lying energy levels of a superfluid  $^4\text{He}$  system exhibit a characteristic grouping behavior. One might naturally wonder whether this behavior is dependent solely on the periodic boundary condition of the system under analysis. However, further examination reveals that this is not necessarily

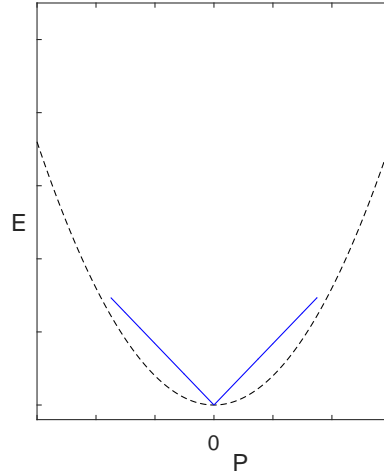


**Figure 6.** The blue lines in the figure represent the linear dispersions of  $grp_0$ , while the dashed parabola corresponds to the energy-momentum relation  $E(P) = E_g + P^2/2NM$ . Since all energy levels of the system must be located above the parabola, the blue lines cannot extend further to cross the curve. As a result, the dispersion behavior must be adjusted at large  $|P|$  regions so that the extended dispersion lines can remain above the parabola, as shown in Fig. 7(a).

the case.

In reality, it is generally unreasonable to assume that an intrinsic property of a physical system is dependent upon its boundary conditions. In the context of  $^4\text{He}$  superflow, a closed system naturally possesses a periodic boundary condition, whereas an open system can be deemed a part of a closed system (see Fig. 5), indicating that both systems possess the same fundamental properties.

Upon closer examination, one can realize that the grouping of low-lying energy levels in superfluid  $^4\text{He}$  is attributed to two fundamental physical factors: Galilean invariance and the discreteness of single-particle orbits carrying momentum along the superflow direction, which arises from the finite dimensions of the system [45]. As both open and closed systems possess these two factors, thus intrinsically possessing the same grouping property. While the periodic boundary condition of a closed system provides a more straightforward means of demonstrating this property from a formal standpoint, the boundary condition of an open system may introduce additional formal complexity.

## VI. Velocity dependence of the thermal energy of a superflow

The preceding section expounded on the grouping behavior of microscopic levels of superfluid  $^4\text{He}$ . It is evident that the system's macroscopic properties are statistically determined by the occupied group(s) and naturally have a dependence on the group(s). In this regard, we shall examine two important properties: the superflow velocity and the thermal energy (density).

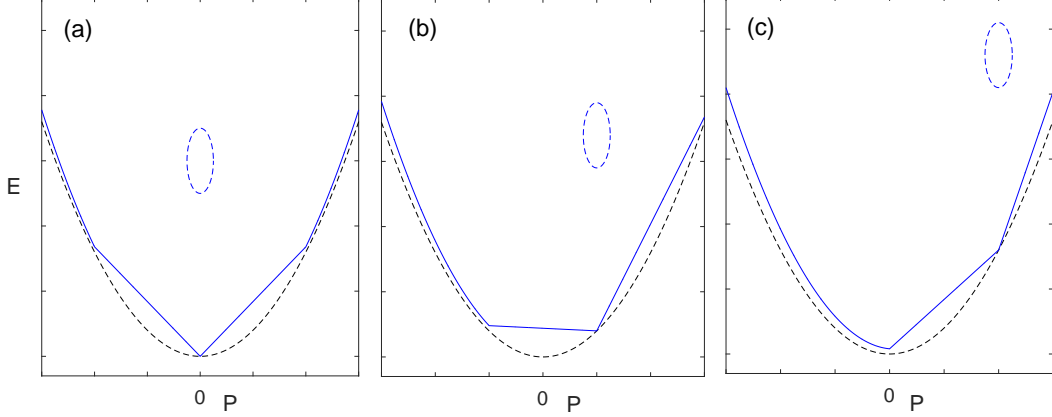


**Figure 7.** (a) The magnitude of the slope of the linear dispersion line of  $grp_0$  remains constant. The dashed parabola corresponds to the energy-momentum relation  $E(P) = E_g + P^2/2NM$ . Panels (b) and (c) show two Galilean transformations of  $grp_0$ , corresponding to superflow states with middle and large flow velocities, respectively. The ellipse in panel (a) roughly denotes the region of dense energy levels that make the major contribution to the system's thermal energy at a given temperature. In panels (b) and (c), the ellipse region is raised, and the dense levels in this region are less involved in the contribution to the thermal energy, resulting in a decrease in the thermal energy of the system.

To further characterize the group  $grp_k$ , a velocity parameter  $v_k$  can be defined as:

$$v_k = 2\pi\hbar k / ML. \quad (9)$$

This parameter corresponds to the center-of-mass velocity of the microscopic state with a wavefunction of  $e^{\sum_{j=1}^N i2\pi k x_j / L} \psi_g$ , which belongs to the group  $grp_k$ .

The thermally averaged velocity of the system in the group  $grp_k$  is determined by:

$$\bar{v}_{grp_k}^T = \frac{\sum_{\phi_\gamma \in grp_k} \langle \phi_\gamma | \frac{\hat{P}_x}{NM} | \phi_\gamma \rangle e^{\frac{-E_\gamma}{kT}}}{\sum_{\phi_\gamma \in grp_k} \langle \phi_\gamma | \phi_\gamma \rangle e^{\frac{-E_\gamma}{kT}}}. \quad (10)$$

The superflow velocity is clearly represented by  $\bar{v}_{grp_k}^T$ , which possesses a temperature dependence and can differ significantly from  $v_k$ . Empirical evidences from superfluid  $^4\text{He}$  indicate that  $v_k$  can reach velocities several tens of meters per second or more, while the corresponding  $\bar{v}_{grp_k}^T$  at temperatures well below the transition point is generally two orders of magnitude smaller. Moreover,  $\bar{v}_{grp_k}^T$  approaches zero near the transition point, whereas  $v_k$  remains independent of temperature. At a specific temperature (above 1 K),  $\bar{v}_{grp_k}^T$  increases with the group number  $k$  and may be used to distinguish the groups. Consequently, other group-specific properties of the system can be regarded as being flow-velocity dependent. We shall investigate the flow-velocity dependence of the superflow's thermal energy.

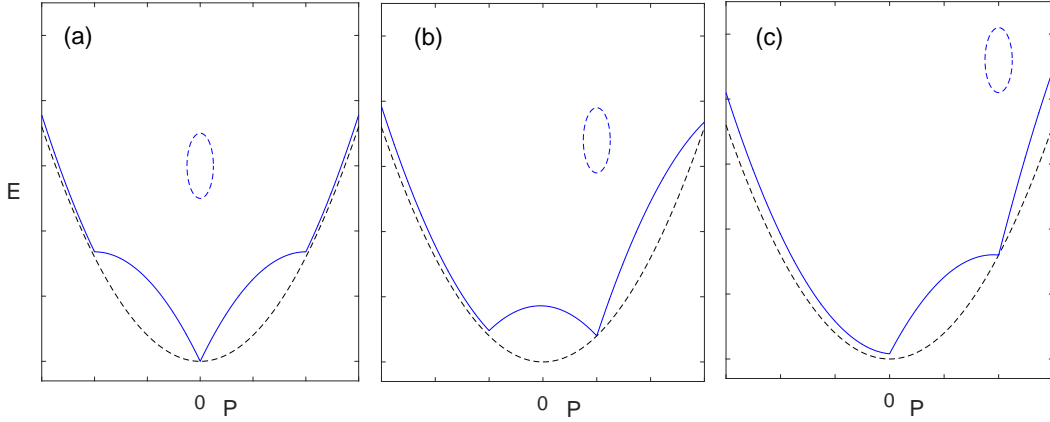


**Figure 8.** The dispersion of  $grp_0$  in this figure differs from that in Fig. 7(a). At small momentum values, the dispersion is linear, although the magnitude of the slope decreases as  $|P|$  increases. Panels (b) and (c) display two Galilean transformations of  $grp_0$ .

The thermal energy of the system in the group of  $grp_k$  is formally calculated as follows:

$$\overline{E}_{grp_k}^T = \frac{\sum_{\phi_\gamma \in grp_k} \langle \phi_\gamma | E_\gamma | \phi_\gamma \rangle e^{-\frac{E_\gamma}{kT}}}{\sum_{\phi_\gamma \in grp_k} \langle \phi_\gamma | \phi_\gamma \rangle e^{-\frac{E_\gamma}{kT}}}. \quad (11)$$

In order to perform a qualitative analysis of  $\overline{E}_{grp_k}^T$ , it is imperative to possess a comprehensive understanding of the level distributions of  $grp_k$  in the momentum-energy plane. One can acquire this knowledge by investigating solely the level distributions of  $grp_0$ , as  $grp_k$  can be considered a Galilean transformation of  $grp_0$ . In Fig. 2, only a subset of levels within  $grp_0$  is schematically plotted, where the lower boundaries are presented by two approximately linear dispersions. However, this linearity breaks down at high momentum regimes for a fundamental reason. In Fig. 6, the linear boundaries of  $grp_0$  are plotted alongside a parabolic curve, defined as  $E = E_g + P^2/2NM$ . It can be realized that no microscopic levels of the system can exist below this parabolic curve. This can be proven using the method of proof by contradiction method to illustrate this point. Suppose there exists an eigenstate with an wavefunction  $\psi_\zeta$ , which has a momentum of  $P_\zeta$  and has an energy  $E_\zeta < E_g + P_\zeta^2/2NM$ . Then, one can find an integer  $n$  such that  $n \leq -\frac{P_\zeta L}{2\pi\hbar} < n+1$ . then the state described by the wavefunction  $\psi_\zeta^{cmn} = e^{\sum_{j=1}^N i2\pi n x_j/L} \psi_\zeta$  will have a momentum very close to zero, and its energy will be approximately  $E_\zeta^{cmn} = E_\zeta - P_\zeta^2/2NM$ , which is smaller than  $E_g$ . This contradicts the fact that the lowest eigen energy should be  $E_g$ .

In Fig. 7(a), a possible scenario for the dispersion behavior of  $grp_0$  is presented where the magnitude of the slopes of the linear dispersion remains constant until it approaches the parabola. On the other hand, Fig. 8(a) illustrates another possible

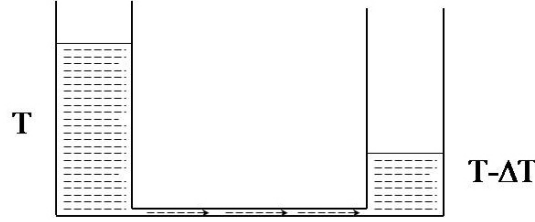


**Figure 9.** The mechano-caloric effect of superfluid  $^4\text{He}$ . The superflow exhibits a high flow velocity and low thermal energy density in the narrow channel. As the superflow exits the channel, it transitions to a state of vanishing flow velocity and a correspondingly high thermal energy density, assuming that the temperature remains constant. The conservation of energy dictates that a drop in temperature is required to compensate for the energy lost due to the reduction in flow velocity.

scenario where the magnitude of the slopes of the linear dispersion decreases with  $|P|$  until it approaches the parabola.

After qualitatively illustrating the behavior of the lower boundaries of  $grp_0$  in the momentum-energy plane, it is imperative to analyze the level density of  $grp_0$  at various locations in the same plane. Notably, the region proximate to the group's lower boundary exhibits a relatively sparse distribution of levels. In contrast, levels are considerably more concentrated in the central region around  $P \approx 0$ , particularly at higher energies (with the extent of the high-energy region dependent on temperature). When considering the Boltzmann factor  $e^{-E/kT}$ , it is evident that the levels enclosed by the ellipse in Fig. 7(a) (and Fig. 8(a)) primarily contribute to the system's thermal energy. Conversely, the contribution from the scarce levels in the remaining region is comparatively insignificant.

When  $grp_0$  is transformed into  $grp_k$  (as plotted in Figs. 7 and 8), it becomes apparent that the region of high level-density is displaced towards the right ( $k > 0$ ) and is elevated by an energy quantity of approximately  $\Delta E = 1/2NMv_k^2$ , as indicated by Eq. 5. Concurrently, the sparse regions located near the left boundary of  $grp_0$  are shifted towards lower energies. The upliftment of the high level-density region leads to its reduced contribution to the thermal energy as a result of the Boltzmann factor in Eq. 11, thereby resulting in a decrease in the value of  $E_{grp_k}^T$  due to the diminishing major part.  $E_{grp_k}^T$  is a decreasing function of  $|v_k|$  or  $|k|$  owing to the upliftment of the high level-density region.

The energy difference  $\Delta E$  is  $1.3 \times 10^{-24}$  J per atom at  $v_k = 20\text{m/s}$ , and  $12 \times 10^{-24}$  J per atom at  $v_k = 60\text{m/s}$ . At  $T = 1.6\text{K}$ , the average thermal energy of a static superfluid  $^4\text{He}$  is roughly  $2.6 \times 10^{-24}$  J per atom, while at  $T = 1.8\text{K}$ , it is about  $5.6 \times 10^{-24}$  J per atom. A comparison of these values suggests that the contribution of the high level-density region to the thermal density becomes effectively negligible when  $v_k$  is sufficiently large. The thermal energy density of a superflow can decrease



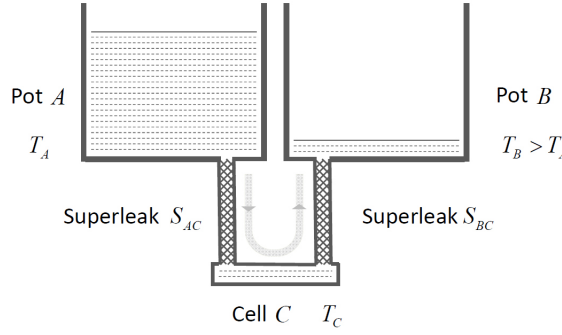


**Figure 10.** A schematic plot of superflow system.

by several orders of magnitude as the flow velocity increases, which is a remarkable quantum property of superfluid  $^4\text{He}$ .

The mechano-caloric effect of superfluid  $^4\text{He}$  (see Fig. 9) can be naturally explained in the light of the velocity dependence of the thermal energy. Notably, when there is a substantial variation in the flow velocity of a superflow, the associated thermal energy experiences significant perturbation. The fundamental principle of energy conservation necessitates a corresponding adjustment in the temperature of the superflow to compensate for the energy variation caused by the flow velocity change. This intrinsic coupling between the variations in flow velocity and temperature reflects the group-specific nature of the system's thermal states.

## V. Experimental observations of a self-heating effect of $^4\text{He}$ superflows

In this section, we present experimental observations of a self-heating phenomenon of  $^4\text{He}$  superflows, which corroborates that  $^4\text{He}$  superflows carry thermal energies. This counter-intuitive heating effect bears a phenomenological resemblance to the Peltier effect of electric current across two distinct conductors.

The main setup of the superflow system is schematically plotted in Fig. 10. The system comprises three interconnected vessels, namely, pot  $A$ , pot  $B$ , and cell  $C$ , which are arranged in series using two superleaks, labeled as  $S_{AC}$  and  $S_{BC}$ . Cell  $C$  is thermally isolated from its surroundings except for its thermal links to the pots via the superleaks.

The experimental procedure involves initially filling pot  $A$  with superfluid  $^4\text{He}$  and subsequently establishing superflows through  $S_{AC}$ , cell  $C$ , and  $S_{BC}$  by setting a positive temperature difference between pot  $B$  and  $A$  (*i.e.*, the fountain effect), resulting in the transportation of superfluid from pot  $A$  to  $B$ . One would expect that the temperature of cell  $C$  ( $T_C$ ) would stabilize between the temperatures of pot  $B$  ( $T_B$ ) and pot  $A$  ( $T_A$ ). However, observations indicate that superflows can significantly heat cell  $C$ , resulting in a steady-state value of  $T_C$  that exceeds  $T_B$  by over one hundred millikelvins.

The experiment is carried out on a two-stage Gifford-McMahon refrigerator with

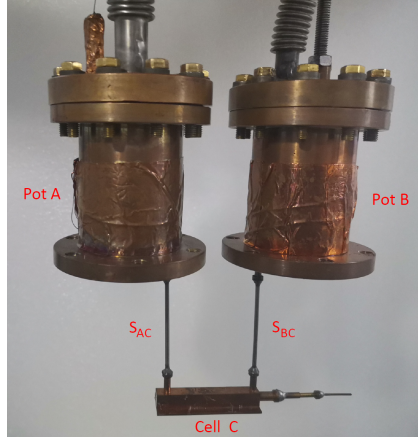


**Figure 11.** A picture of superflow system.  $S_{AC}$  and  $S_{BC}$  refer to the superleaks.

a cooling power of  $1\text{ W}$  at  $4.2\text{ K}$ , and a base temperature of  $2.4\text{ K}$ . To reach the superfluid temperature regime, a liquid  $^4\text{He}$  cryostat is constructed based on the scheme provided in Ref. [46]. The cryostat involves a stainless steel capillary, which has an inner diameter (i.d.) of  $0.18\text{ mm}$ , an outer diameter (o.d.) of  $0.4\text{ mm}$ , and a length of  $1\text{ m}$ , which acts as the Joule-Thomson impedance. A copper pot with an i.d. of  $4.0\text{ cm}$  and a volume of  $78\text{ cm}^3$  is used to collect liquid  $^4\text{He}$  and serve as pot  $A$  of the superflow system. Another identical copper pot is employed as pot  $B$ . The inner cavity of cell  $C$ , made of a small copper block, is predominantly cylindrical with a diameter of  $3\text{ mm}$  and a length of  $40\text{ mm}$ . Two superleaks are made of stainless steel tubes packed with jeweler's rouge powder (with an average particle size of  $70\text{ nm}$  determined by TEM). The tube for  $S_{AC}$  has an i.d. of  $0.8\text{ mm}$ , an o.d. of  $2.0\text{ mm}$ , and a length of  $65\text{ mm}$ , while the tube for  $S_{BC}$  has an i.d. of  $1.0\text{ mm}$ , an o.d. of  $2.0\text{ mm}$  and a length of  $65\text{ mm}$ . The two superleaks are soft soldered to cell  $C$ , and they are positioned such that the lower end of each superleak is situated near one end of cell  $C$ 's cylindrical cavity (see Fig. 11). The upper end of  $S_{AC}$  is connected to pot  $A$ , and the upper end of  $S_{BC}$  is connected to pot  $B$ .

A combination of copper braids and brass strips is used as a thermal link to connect pot  $A$  with a cooling plate mounted directly on the second stage of the refrigerator. This thermal link has a thermal conductance of approximately  $2\text{ mW/K}$  at  $2\text{ K}$ . On the other hand, the main thermal link between pot  $B$  and its surroundings is a copper braid connecting the two pots. Resistance wires are wrapped around both pots to serve as heaters. Pot  $A$  and pot  $B$  are fitted with pumping lines and valves to regulate the pumping rate, providing a further method for the temperature controls of the pots. Calibrated carbon ceramic resistances [47] are used as temperature sensors to measure  $T_A$ ,  $T_B$  and  $T_C$ , with an accuracy of  $5\text{ mK}$  below  $2.5\text{ K}$ . The dissipation power of temperature sensor on cell  $C$  is kept significantly below  $10^{-7}\text{ W}$ , ensuring that its heating effect is limited.

The refrigerator is equipped with two radiation shields, which are composed of

$T_A$ (K)	$T_B$ (K)	$T_C$ (K)
1.500(4)	1.700(4)	1.847 (1)
1.600(4)	1.800(4)	1.927 (1)
1.600(4)	1.900(4)	2.014 (1)

**Table 1.** Steady values of  $T_C$  at various combinations of  $T_A$  and  $T_B$ . The number in the parenthesis denotes the fluctuation amplitude of the measured temperature over several hours.  $T_C$  is observed to be highly stable, with an deviation no larger than 1 mK.

copper and coated with a thin layer of nickel. These shields are installed in each of the two stages of the refrigerator, respectively. One shield operates at a temperature of approximately 45 K, while the other shield maintains a temperature below 2.8 K. Great care is made to shield cell  $C$  from exposure to thermal radiation that originate from sources with a temperature exceeding 3 K.

To initiate the accumulation of liquid  $^4\text{He}$  (with a purity of 99.999%) in pot  $A$ , the temperature  $T_A$  is deliberately raised above the  $\lambda$  point, which prevents superflow through the superleak  $S_{AC}$ , while simultaneously allowing cell  $C$  and pot  $B$  to remain unoccupied. After a substantial amount of liquid  $^4\text{He}$  has accumulated in pot  $A$ , the pumping rate is adjusted to lower  $T_A$ . As  $T_A$  drops below the  $\lambda$  point, superflow is initiated through the superleak  $S_{AC}$ , filling cell  $C$  in the process. Establishing the superfluid transport from pot  $A$  to pot  $B$  via cell  $C$  can be accomplished by setting  $T_B$  higher than  $T_A$ . This transport can be sustained for several hours. During this transport process, it is observed that  $T_C$  remains stable once it reaches a steady value. Tab. 1. lists the various stable values of  $T_C$  for different predetermined combinations of  $T_A$  and  $T_B$ .

A heating process of cell  $C$  is plotted in Fig. 12. At the initial moment presented in the figure, pot  $A$  contains liquid  $^4\text{He}$  with a temperature above the  $\lambda$  point, while both pot  $B$  and cell  $C$  are empty. Thereafter, pot  $A$  is pumped and its temperature decreases, which causes an accompanying drop in  $T_B$  due to the relatively large thermal link between the two pots. At a certain point, the resistance wire around pot  $B$  is activated, which stabilizes  $T_B$  at a set value of 1.85 K.

As  $T_A$  decreases,  $T_C$  also decreases. Once both temperatures dip below the  $\lambda$  point, superfluid transport between pot  $A$  and cell  $C$  is initiated, which plays a crucial role in determining the value of  $T_C$  relative to  $T_A$ .  $T_C$  remains a few millikelvins below  $T_A$  during the period of superfluid filling of cell  $C$ . The difference between  $T_C$  and  $T_A$  remains relatively locked owing to a negative feedback mechanism. Specifically, if  $T_C$  falls further below  $T_A$ , the fountain pressure of the superfluid that stems from the temperature difference between  $T_A$  and  $T_C$  overcomes the gravitational pull and directs the superfluid back from cell  $C$  to pot  $A$ , thereby elevating  $T_C$ . Conversely, if  $T_C$  approaches  $T_A$ , the overall force, which comprises both fountain pressure and gravitational pull, conducts the superflow from pot  $A$  to cell  $C$ , leading to a reduction in  $T_C$ .

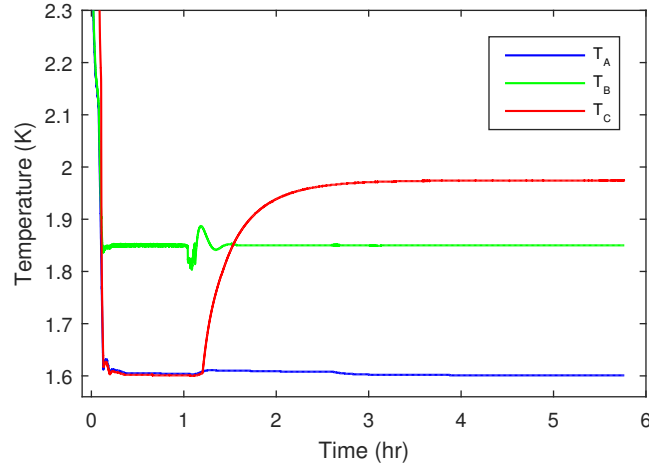


**Figure 12.** A heating process of cell  $C$ . Note that after reaching a steady state, the temperature of cell  $C$  exhibits a high degree of stability.

When the filling of cell  $C$  reaches near completion, the initiation of superfluid transport between cell  $C$  and pot  $B$  causes significant fluctuations of  $T_B$ , which oscillates several times within a period of around thirty minutes. The underlying cause of these fluctuations is the relatively small heat capacitance of the initially empty copper pot  $B$ . The introduction of even a small amount of cold superfluid  $^4\text{He}$  into pot  $B$  can provoke a considerable variation of  $T_B$ , and the temperature stabilization system cannot respond in a timely manner. As a certain amount of superfluid  $^4\text{He}$  accumulates in pot  $B$ , subsequent injections of cold superfluid no longer produce dramatic change in  $T_B$ , thus enabling the temperature stabilization of  $T_B$  to be restored.

Once the transport of superfluid  $^4\text{He}$  through these two superleaks is fully established,  $T_C$  increases steadily and reaches a value 120  $mK$  above  $T_B$ , which demonstrates a counter-intuitive heating phenomenon. The data presented in Fig. 12 allows for useful estimations of the heating powers received by cell  $C$  at two distinct stages. During the first stage, which takes approximately an hour and corresponds to the filling of superfluid into cell  $C$ , the cell receives heat transfer from pot  $B$  via thermal conduction while being cooled by the influx of superfluid (note that this heat transfer drives superfluid to flow into cell  $C$ ). The heat received by cell  $C$  during this stage corresponds to the thermal energy of liquid  $^4\text{He}$  with a volume of 0.1  $c.c$  at a temperature of 1.6  $K$ , resulting in a heating power denoted by  $P_{stage1}$  of approximately 1.5  $\mu W$ . Right after the first stage, the temperature of cell  $C$  (superfluid filled) rises from 1.6  $K$  to 1.85  $K$  over a duration of 20 minutes, which is considered as the second stage. The heat received during this stage corresponds to roughly the change of thermal energy of liquid  $^4\text{He}$  in the cell, resulting from the temperature change from 1.6  $K$  to 1.85  $K$ . The heating power denoted by  $P_{stage2}$  is 7.3  $\mu W$ .

It is worth noting that even if cell  $C$  could experience some abnormal background heating during the experiment, this heating should also be present in the first stage as

well and thus has a smaller power than  $P_{stage1}$ . Based on the fact that  $P_{stage2} > 4P_{stage1}$ , it is concluded that the major portion of  $P_{stage2}$  is sourced from the superflows rather than some abnormal heating background. The superflows remain responsible for the heating of cell  $C$  for the rest of the time presented in Fig. 12. Since the superflows' negligible kinetic energies are negligible, it can be inferred that the heating resulting from the superflows must originate from their thermal energies.

The observed heating phenomenon of superflows is somehow analogous to the Peltier effect, which occurs when an electric current flows across two distinct conductors. Specifically, in this phenomenon, the thermal energy density of the inlet superflow entering cell  $C$  is larger than that of outlet superflow exiting the cell, resulting in the heating of the cell. Fundamentally, the difference between the inlet and outlet superflows' thermal energy densities is attributed to the velocity dependence of a superflow's thermal energy.

The velocity behavior of the superflows in the two superleaks is complex, as they are frictionless and lack a means of stabilizing their velocities. The superflow in superleak  $S_{AC}$   $^4\text{He}$ s continuous acceleration or deceleration due to pressure difference between superfluid in pot  $A$  and that in cell  $C$ , wherein the fountain pressure, resulting from the temperature difference across  $S_{AC}$ , comprises a significant part of the overall pressure difference. The pressure in cell  $C$  can abruptly rise as it transitions from a nearly full state to a fully filled state, which regulates the velocity of inlet superflow and prevents it from attaining high velocity. On the other hand, the pressure increase in cell  $C$  can accelerate the outlet superflow, causing it to reach a large velocity regime. Furthermore, if  $T_C > T_B$ , the superflow in  $S_{BC}$  can reverse its flow direction when cell  $C$  deviates from a fully filled state, leading to a shorter actual flow time of the outlet superflow than that of the inlet superflow. These analyses indicate an asymmetry between the velocity distributions of the inlet and outlet superflows, resulting in a disparity in their thermal energies.

To corroborate our findings, we conducted a comparative experiment in which we replaced the superleak  $S_{BC}$  by a solid rod of stainless steel of similar dimensions (radius of 2.0 mm and a length of 65 mm). This experiment only allows superfluid transport between pot  $A$  and cell  $C$  while it is obstructed between cell  $C$  and pot  $B$ . As anticipated, and confirmed, the steady value of  $T_C$  is well between  $T_A$  and  $T_B$ . The comparison provides additional robust evidence that the unusual heating phenomenon is not due to some abnormal background heating.

In earlier experiments, it appears that  $^4\text{He}$  superflows carry negligible thermal energies. This observation is commonly attributed to the absence of controlled superflow velocities, which often approaches the critical value during the experimentation. However, in the contrast to those experiments, the present investigation involves a partial control of the superflow velocities, leading to the observation of an intriguing heating phenomenon.

## VI. Conclusions and perspectives

Superfluid  $^4\text{He}$  is one of the most fascinating systems in condensed matter physics, and it continues to unveil surprising quantum behaviors more than eight decades after the discovery of superfluidity. Despite substantial efforts in the past, however, the exact microscopic understanding of this system had remained elusive owing to the complexity of the many-body quantum problem.

This paper presents a fundamental property of the quantum system of superfluid  $^4\text{He}$ , specifically, the grouping behavior of its low-lying levels. Based on this observation, we offer a natural explanation of superfluidity. Furthermore, we demonstrate that the group-specific nature of the thermal equilibrium state of a superflow leads to another intriguing feature of this system: the thermal energy density of a superflow at a given temperature depends on its velocity, with higher velocities leading to lower thermal energy density. This fundamental connection between the thermal and hydrodynamic properties of the system plays an essential role in various phenomena, such as the mechano-caloric effect. We also provide a natural explanation for the presence of dissipation in a superflow undergoing time-varying motion, in contrast to steady motion. In addition, we suggest that several condensed-matter systems, which exhibit interesting low temperature phases described an order parameter, share the same common microscopic basis: their low-lying quantum states are grouped. Each group of quantum levels can produce a distinct macroscopic thermal state of the system with a particular value of the order parameter.

Drawing inspiration from the theoretical findings, we conducted an experiment to investigate  $^4\text{He}$  superflows, which led to the observation of a counter-intuitive heating phenomenon. Our results confirm that a superflow can carry considerable thermal energy, related to its flow velocity.

The theoretical picture of superfluid  $^4\text{He}$  presented in this paper has the potential to shed light on some other intriguing phenomena that have not yet been fully elucidated in the system. Additionally, it can lead to predications of a couple of novel quantum behaviors which can be investigated empirically. A thorough integration of theoretical and experimental aspects in this field can be pursued based on this picture, which will reinforce the conviction that quantum mechanics offers a definitive account of laboratory systems.

## References

- [1] P. Kapitza, *Nature* **141**, 74 (1938).
- [2] J. F. Allen & A. D. Misener, *Nature* **141**, 75 (1938).
- [3] J. F. Allen & H. Jones, *Nature* **141**, 243 (1938).
- [4] J. G. Daunt & K. Mendelssohn, *Nature* **143**, 719 (1939).
- [5] L. Landau, *J. Phys. USSR* **5**, 71 (1941).
- [6] L. Landau, *J. Phys. USSR* **11**, 91 (1947).
- [7] N. Bogoliubov, *J. Phys. USSR* **11**, 23 (1947).
- [8] F. London, *Nature* **141**, 643 (1938).

- [9] F. London, Phys. Rev. **54**, 947 (1938).
- [10] L. Tisza, Nature **141**, 913 (1938).
- [11] F. Bloch, Phys. Rev. **A 7**, 2187 (1973).
- [12] A. G. Leggett, Rev. Mod. Phys. **73**, 307 (2001).
- [13] R. Feynman, R. B. Leighton & M. L. Sands, The Feynman Lectures on Physics, vol. III, chapter 4, Addison-Wesley, Reading, MA (1965).
- [14] D. R. Tilley & J. Tilley, Superfluidity and Superconductivity, A. Hilger, 1986.
- [15] D.V. Osborne, Proc. Phys. Soc. A **63**, 909 (1950).
- [16] E. L. Andronikashvili & I. P. Kaverlin, J. Exp. Theor. Phys. U.S.S.R., **28**, 126 (1955).
- [17] K. R. Atkins, Proc. Roy. Soc. A **203**, 240 (1950).
- [18] G. S. Picus, Phys. Rev. **94**, 1459 (1954).
- [19] F. D. Manchester, Can. J. Phys. **33**, 146 (1955).
- [20] H. Seki, Phys. Rev. **128**, 502 (1962).
- [21] F. I. Glick & J. H. Werntz, Jr., Phys. Rev. **178**, 214 (1969).
- [22] E. F. Hammel, W. E. Keller & R. H. Sherman, Phys. Rev. Lett. **24**, 712 (1970).
- [23] J. S. Brooks & R. B. Hallock, Phys. Lett. A **63** 319 (1977).
- [24] J. P. Turneaure & I. Weissman, J. App. Phys. **39** 4417 (1968).
- [25] M. Tinkham, Introduction to superconductivity, Dover, New York (1996).
- [26] R. D. Puff & J. S. Tenn, Phys. Rev. A **1**, 125 (1970).
- [27] O. Harling, Phys. Rev. A **3**, 1073 (1971).
- [28] L. J. Rodriguez, H. A. Gersch & H. A. Mook, Phys. Rev. A **9**, 2085 (1974).
- [29] E. C. Svensson, V. F. Sears & A. Griffin, Phys. Rev. B **23**, 4493 (1981).
- [30] V. F. Sears, E. C. Svensson, P. Martel, & A. D. B. Woods, Phys. Rev. Lett. **49**, 279 (1982).
- [31] E. C. Svensson & V. F. Sears, Physica **137B**, 126 (1986).
- [32] D. M. Ceperley & E. L. Pollock, Can. J. Phys. **65** 1416 (1987).
- [33] A. Whitlock & R. M. Panoff, Can. J. Phys. **65**, 1409 (1987).
- [34] T. R. Sosnick, W. M. Snow, P. E. Sokol & R. N. Silver, Europhys. Lett. **9**, 707 (1990).
- [35] H. R. Glyde, R. T. Azuah & W. G. Stirling, Phys. Rev. B **62**, 14337 (2000).
- [36] S. Moroni & M. Boninsegni, J. Low Temp. Phys. **136**, 129 (2004).
- [37] M. Boninsegni, N. V. Prokof'ev & B. V. Svistunov, Phys. Rev. E **74**, 036701 (2006).
- [38] R. Rota & J. Boronat, J. Low Temp. Phys. **166** 21 (2012).
- [39] T. R. Prisk, M. S. Bryan, P. E. Sokol, G. E. Granroth, S. Moroni & M. Boninsegni, J. Low Temp. Phys. **189** 158 (2017).
- [40] G. D. Mahan, Many-Particle Physics, third edition, chapter 11, Kluwer Academic/Plenum Publishers, New York (2000).
- [41] H. R. Glyde, Rep. Prog. Phys. **81** 014501 (2018).
- [42] Y. Yu, Ann. Phys. **323**, 2367 (2008), and references therein.
- [43] Y. Yu, Mod. Phys. Lett. **B 29**, 1550068-1 (2015).
- [44] J. D. Reppy & D. Depatie, Phys. Rev. Lett., **12**, 187-189 (1964).
- [45] Practically, any sample of superfluid  $^4\text{He}$  in a laboratory has a finite size. However, the system with  $N \rightarrow \infty$  in the thermodynamic limit can be obtained from a finite-sized system through appropriate scaling, which preserves its inherent physical properties.
- [46] A. DeMann, S. Mueller & S. B. Field, Cryogenics, **73**, 60 (2016).
- [47] <https://www.temati-uk.com/>.
- [48] The average rate of transfer of superfluid  $^4\text{He}$  from pot  $A$  to pot  $B$  ranges between 3 to 4 cubic centimeters per hour. The flow velocities through superleaks are typically a few millimeters per second. The associated kinetic energy per  $^4\text{He}$  atom is approximately  $10^{-29}$  Joule, corresponding to a temperature scale of  $1 \mu\text{K}$ , which is negligible for a  $^4\text{He}$  system operating above  $1.6 \text{ K}$ . Furthermore, as discussed later in the manuscript, the inlet superflow exhibits a smaller velocity than the outlet superflow. Consequently, any change in the kinetic energy of the superflows will result in a minor cooling effect on cell  $C$  rather than a heating effect.